Rotation of Crustal Blocks in Central California based on Paleomagnetic Declination

Zachary J. McGuire
Senior Integrative Exercise
March 10th , 2008

Submitted in partial fulfillment of the requirements for a
Bachelor of Arts degree from Carleton College, Northfield, Minnesota.

Table of Contents

Rotation of Crustal Blocks in Central California based on Paleomagnetic Declination

Zachary J. McGuire
Carleton College
Senior Integrative Exercise
March 10, 2007

Advisor:
Sarah Titus, Carleton College

ABSTRACT

The Rinconada fault is a strand of the San Andreas fault system in central California. Paleomagnetic declinations from specimens at 27 sites within 10 km of the fault had a mean clockwise vertical axis rotation of 11.3±8.8˚. These 27 sites were grouped geographically into four regions lateral along the Rinconada fault that indicated mean vertical axis rotations ranging from 3.8˚ counterclockwise to 17.0˚ clockwise. In addition, 15 sites west of the Rinconada fault were rotated 20.5±9.3˚ while sites east of the Rinconada fault were rotated clockwise only 2.1±11.0˚. The results from this study can best be explained by several small, localized crustal blocks that have reacted differently to the deformation associated with the Rinconada fault. This is supported by analysis of fold axis obliquity of mapped folds within the region that indicate regional differences between the same regions. Overall rotation of crustal blocks near the Rinconada fault is evidence that some degree of fault parallel motion is accommodated via distributed deformation off the fault in this transpressional setting.

Keywords: Paleomagnetism; Transpression; Vertical Axis Rotation; Central California, Rinconada fault

1. Introduction

Prior to 30 million years ago the western coast of North America was a convergent plate boundary with a classic volcanic arc. Collision between this island arc, oceanic sediment and the North American craton extended the continental margin to its present location (Burchfiel, 1970). As a result, modern California is a stitched together composite of accreted sedimentary terranes and igneous intrusions that date back to the Cretaceous (Beck, 1980). The present plate configuration- featuring a major dextral transform margin- began at a maximum of 30 Ma after subduction of the Farallon plate brought the Pacific Plate and North American Plate into contact (Atwater, 1970). The San Andreas fault system represents the plate boundary between the North American Plate and Pacific Plate; the relative plate motions of which are accommodated as dextral slip along the fault (McKenzie and Parker, 1967; Morgan, 1968).

Paleomagnetic research has been an instrumental part of understanding the tectonic development of the western margin of North America and, in particular, invaluable for unraveling the complex interactions caused by the development of the San Andreas fault zone in central and southern California (Kamerling and Luyendyk, 1977, 1979; Luyendyk et al. 1980). Other methods of reconstruction have been largely unsuccessful at retracing past movement of tectonic blocks; many of the large rotations discovered in southern California went unnoticed until detection by paleomagnetic methods (Kamerling and Luyendyk, 1977). For example, large paleomagnetic declination anomalies in the Transverse Ranges indicate clockwise crustal blocks rotations of approximately 90˚ (Kamerling and Luyendyk, 1977, 1979; Kamerling et al., 1978; Hornafius, 1985; Luyendyk, 1985). North of the Transverse Ranges, early studies show

little evidence of clockwise crustal block rotations; instead some early work (Terres and Luyendyk, 1985) even suggested small counterclockwise rotations (a feature not predicted by any model of rotation in a dextral system) of less than 10˚.

In this study, we reexamine central California north of the Transverse Ranges, an area that is traditionally thought to be north of the major crustal block rotations. A few of the more recent studies (Omarzai, 1996; Titus et al. 2007) have shown the presence of smaller declination rotations of 10-20˚ clockwise, which indicate that while the tectonic setting may not be analogous to that of the Transverse Ranges, rotation of crustal blocks could still be an important tectonic development in central California.

2. Geologic Setting

2.1- San Andreas fault system

The San Andreas fault system is a group of branching strike-slip faults that extend for approximately 1300 km. The fault system marks the boundary between the Pacific plate and the Sierra Nevadan microplate. The relative plate motion between these two plates is primarily dextral strike-slip with a small component of convergence (Argus and Gordon, 2001) due to a slight angle of obliquity between plate motion and the plate boundary. This combination of strike-slip and convergence is characterized by transpression and accommodates approximately 39 mm/yr of motion through a combination of discrete and distributed deformation (Argus and Gordon, 2001).

The fault system does not appear to be the same everywhere along the plate boundary. In central California (Fig. 1) the San Andreas fault system lacks the branching fault network present in southern California (Dibblee, 1976), where faulting is dominated by

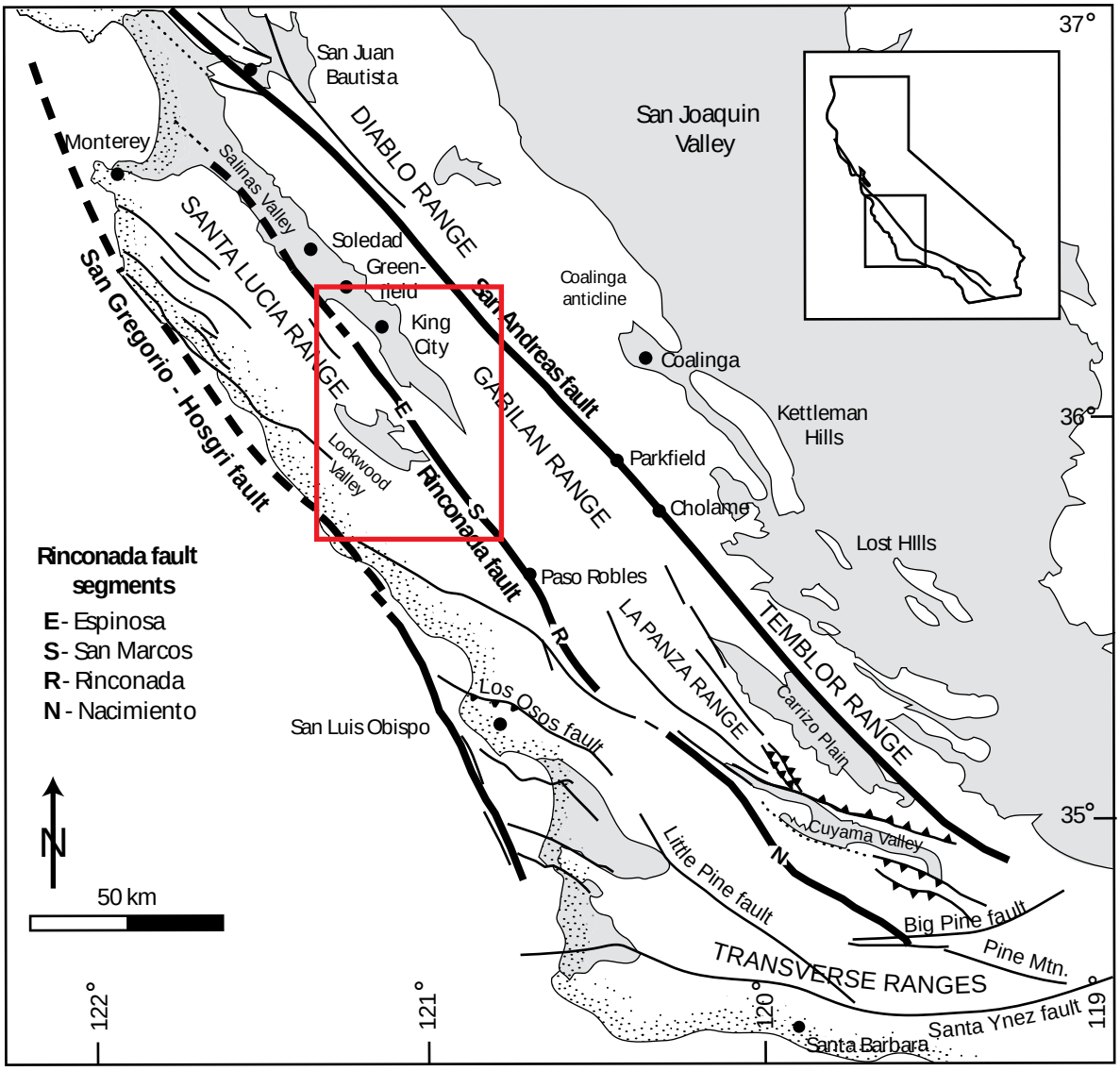

Figure 1. Map of central California with major faults and place names. The red box indicates the field area of this study. Note that fault geometry within and near the field area is dominated bythree parallel faults, the San Andreas, Rinconada, and San Gregorio. Also note that this is not the case south of the study area. Modified from Jennings et al. (1977), Page et al. (1998) and Titus et al. (2007).

right and left lateral faults that are oblique to one another. In central California, the plate boundary is characterized by parallel dextral faults and by series of en echelon folds between these faults that strike NW-SE at a shallow angle to major fault strike.

2.2- Tectonic Development of Central California

The present phase of transpression for the San Andreas fault system is a result of a change in relative plate motion between the North American and Pacific plates that switched from oblique divergence to oblique convergence. The transition from transtension to transpression is contrained by estimates from a number of studies. Argus and Gordon (2001) use predicted rates of uplift of topography on the Coast Ranges as well as total shortening estimates to determine that central California has been in transpression for the last 6 Ma. The authors also use convergence estimates from Jamison (1991) and Namson and Davis (1988) to support a constraint of onset of transpression to approximately 9 Ma. Other studies provide estimates of the onset of transpression that range from 4 Ma (Page, 1981) based on uplift of marine sedimentary units in the Coast Ranges to 8 Ma (Atwater and Stock, 1998). Atwater and Stock's (1998) estimate of uplift is based on plate reconstructions using seafloor magnetic reversals since 33 Ma that indicate a change in relative plate motion azimuth of approximately 23˚ at 8 Ma.

2.3- *Central California Geology*

In central California, there are several parallel faults in the San Andreas fault system that appear to be tectonically related (Dibblee, 1976) based on both their offsets and en echelon positioning (Fig. 1). The San Gregorio-Hosgri and San Gabriel faults are parallel to the Rinconada fault, and are located to the northwest and southeast of the

Rinconada fault, respectively. The Rinconada fault also strikes subparallel and approximately 34 km southwest of the San Andreas Fault.

Folds that are mapped adjacent to the Rinconada fault (Dibblee, 1976) are mostly Pliocene to late Miocene in age. These folds occur in en echelon groups and generally have moderately dipping fold axes (Dibblee, 1976). The folds axes strike NW-SE and strike 12-20˚ oblique to Rinconada fault strike (Mount and Suppe, 1987; Titus et al. 2007).

2.4- Study Area

Samples for this study were collected at sites adjacent to the Rinconada fault, a strand of the San Andreas fault system that is traceable for 250 to 290 km in central California (Fig. 1; Dibblee, 1976). The Rinconada fault is a right lateral strike-slip fault that was the most extensive active fault west of the San Andreas throughout the Miocene and Pliocene (Dibblee, 1976). Although the fault is thought to have been inactive throughout the Holocene and Pleistocene, Pliocene offsets are estimated at 18 km (Dibblee, 1976). Offset from the Early Miocene is not as well constrained, and displacement could be as little as 23 km or as much as 56 km over the last 23 million years, while total displacement since the early Tertiary is as much as 60 km (Dibblee, 1976).

Paleomagnetic sampling of rocks adjacent to the Rinconada fault in this study focuses on rocks of the Monterey Formation, a marine sedimentary package. These sediments were deposited in a number of deep N-S trending coastal basins that formed during the Miocene (Dibblee, 1976; Omarzai, 1996) while central California was still experiencing transtensional relative plate motion. Attempts to age-date deposition via

magnetic reversals yield a deposition window from 17.9 Ma to 11.9 Ma (Omarzai, 1996) for Horse Canyon in the Salinas basin, which coincides with the northernmost sites in this study. The Monterey Formation is predominantly shale, but also includes layers of limestone, dolostone, and chert (Gross,1995).

The Monterrey formation is stratigraphically younger than the early Miocene marine sandstone lithofacies, the Vaqueros Formation. The top of the Monterrey Formation grades into another marine sandstone of Late Miocene age. This facies, the Santa Margarita Formation lies conformably below the Early Pliocene Pancho Rico marine sediments (Dibblee, 1976). The mudstone and shale sedimentary sequence is approximately 960 meters in thickness (measured at Horse Canyon; Omarzai, 1996) and crops out extensively in central and southern California.

3. Paleomagnetism

3.1-Introduction to Paleomagnetism

Paleomagnetic research uses magnetic characteristics of rocks to calculate the direction and degree they have rotated and translated since the magnetic signal was locked into the rock. In order to use the remanent magnetism recorded within rock to estimate rotation and translation, some knowledge of the location of the earth's present and past magnetic pole is necessary. Careful reconstruction of the past magnetic field has resulted in high resolution location of past paleomagnetic poles. The geomagnetic polarity timescale (Vine and Matthews, 1963; Cox et al. 1963, 1964, 1968) links these episodic polar reversals to absolute ages via radiometric dating, resulting in a precise chronology of reversals or "anomalies".

The degree to which a rock stores the magnetic signals is dependent largely on the mineralogy of the rock involved, particularly the presence of Fe or Ti oxides (Butler, 1992). In sediments such as the Monterey Formation, a magnetization is induced at the time of deposition via detrital remanent magnetization (DRM). In this process, ferromagnetic (iron-bearing) detrital minerals align according to the applied magnetic field during accumulation of sediment (Butler, 1992). Primary magnetization (such as DRM) is contrasted by all forms of secondary magnetization, which can occur from exposure to weathering, lightning, or prolonged contact with the present magnetic field.

Methods of demagnetization attempt to isolate the signal of the primary magnetization from any possible secondary magnetizations. In this study, samples were thermally demagnetized by exposing each sample to incrementally higher temperatures approaching the Curie point (the temperature at which a given metal loses ferromagnetic properties). Thermal demagnetization is successful because the decay of stored magnetization signals is temperature dependent. The time needed for a magnetic component signal to decay to zero (known as the "relaxation time") varies by orders of magnitude depending on the grain type (Butler, 1992). Thermal demagnetization subjects samples to temperatures at which the primary and secondary remanent magnetizations begin to rapidly decay (blocking temperatures). Commonly, the features causing secondary magnetization have shorter relaxation times and lower blocking temperatures, meaning that their signals decay at lower temperatures- isolating only the primary remanant magnetization.

Once isolated, the primary remanent magnetization is a vector, conventionally described as the resultant of two component vectors, declination and inclination (Fig. 2).

Inclination describes the vertical component (-90˚ to 90˚) of the primary remanent magnetization and is identified as an angle down from horizontal. Declination describes the horizontal component of magnetization and is described as the angle from geographic north (0˚ to 360˚).

3.2-Methodology

We collected specimens from 69 separate sites covering a broad region adjacent to the Rinconada fault in central California. Between 7 and 15 individual specimens were collected at each site. Sites were chosen based on overall exposure and access to unfractured rock. The majority of sites were therefore road cuts where accurate bedding measurements were possible. Cores were obtained via a gas powered portable drill with a water cooled diamond drill bit and were oriented in the field with a compass.

Paleomagnetic Analyses were performed at the paleomagnetism lab at the University of Western Washington. Samples were thermally demagnetized at incremental temperature steps to eliminate overprinted secondary magnetic signals. Measurement of the magnetic moment of each sample was performed with a Cryogenic Magnetometer and sensed via the Superconducting Quantum Interference Device (SQUID). The specimens were magnetically shielded during storage and sampling to minimize any magnetization that might have occurred after sample collection.

3.3- Data Selection

Rocks from the Monterey Formation typically carry a weak magnetic intensity. In theory, thermally demagnetization eliminates the secondary magnetization and therefore isolates the primary magnetic signal. However, in some specimens, magnetization quickly became too low to interpret over ambient magnetic signals (noise) or

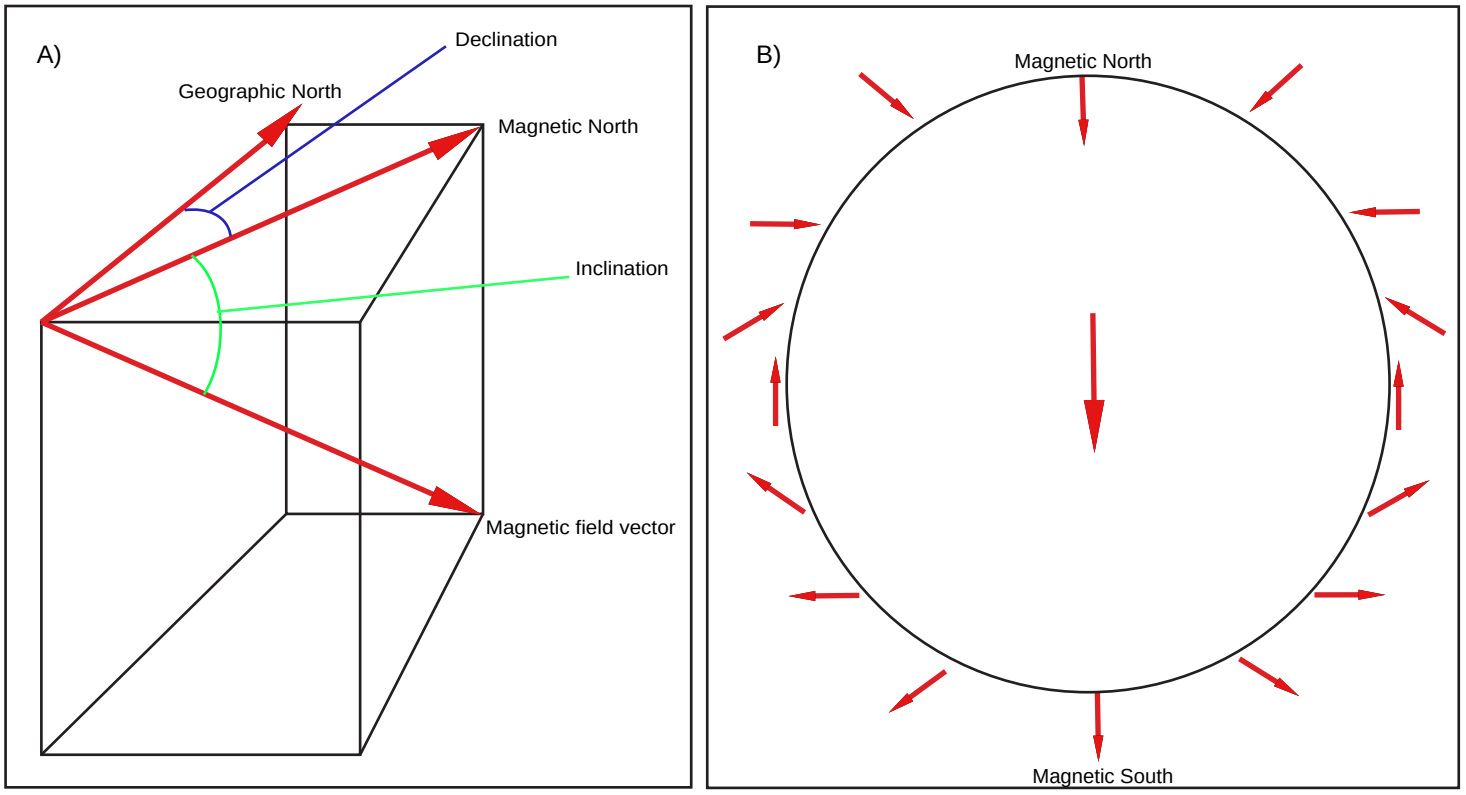

Figure 2. (A) the Magnetic field vector is described by two component angles relative to geographic north. The horizontal component is referred to as the declination (in blue) and the vertical component, measured from horizontal,is referred to as the inclination (in green). In B, a cross-section view of the earth sliced parallel to the magnetic pole illustrates the inclination angle at varying latitudes during normal magnetization.

demagnetization followed no traceable linear path. In other cases, heating caused mineral alignment and remagnetization. Consequently, 42 out of 69 sites were eliminated from this study based on data that was deemed unreliable to uninterpretable. Figure 3 shows examples of both a sample with a good thermal demagnetization pattern and one that has been remagnetized.

The remaining 27 sites have five to seven specimens each, a large enough statistical sampling to generate accurate site means. Of these means, nearly all had an angular 95% confidence area (α95) of <15˚ indicating a fair to good clustering of data points and true mean declinations and inclinations that are well constrained (statistical analyses based on Fisher, 1953).

3.4-Fold Tests

Paleomagnetic declinations and inclinations for each of the 27 sites in this study were converted to site means and clustered into four distinct geographical groups: Greenfield, Quinado Canyon, San Antonio Reservoir and Nacimiento River (Fig. 4). Tilt tests were conducted for each of the four paleomagnetic groups as well as the entire data set. None of these fold tests indicated good clustering at 100% untilting- the expected result for Miocene deposits that predate the predicted Pliocene and Pleistocene folding event(Figures 5-7).

There are, however, a number of indications as to why these fold tests were largely unsuccessful. First, this study covers a large mapped area which suggests a number of regional differences in rotations may have occurred. Non-clustering of site means after untilting may simply reflect rotation amounts that are significantly different across the study area. Second, fold tests cannot account for significant fold plunge, which

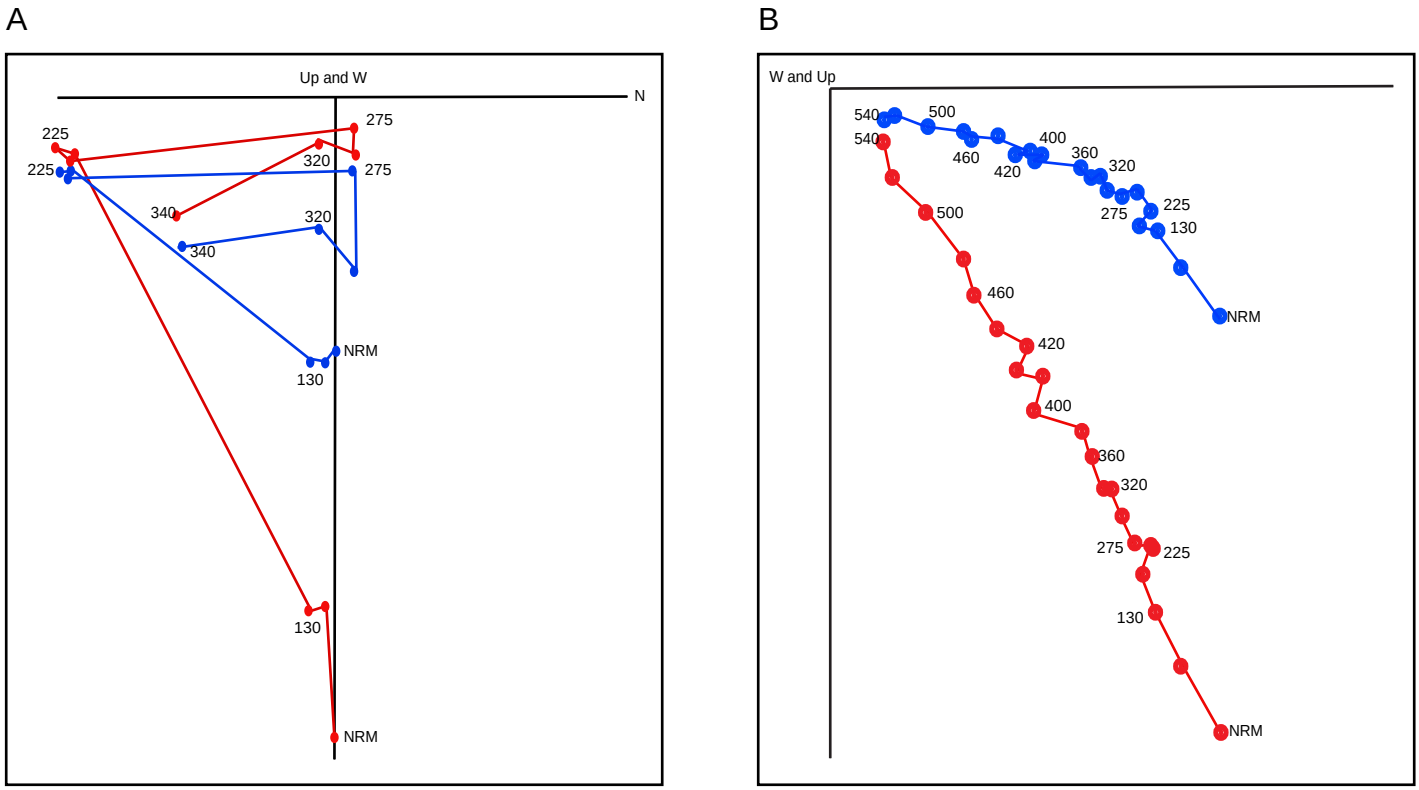

Figure 3. Examples of poor (A) and good (B) results of thermal demagnetization represented by orthogonal vector plots. Blue line indicates declination and red line indicates inclination. Notice that in A, progressive demagnetization does not move towards the origin. There is also no clear direction of demagnetization. This sample has probably been remagnetized during thermal heating steps. In B, the signal exhibits a clear path of demagnetization, as well as a slight change of direction at approximately 320 degrees C. This sample's signal is decaying to zero towards the origin, indicating that the samples' magnetic signal is decreasing to zero with increased heat.

may introduce error into the results of the fold tests. For these reasons, the failure of the fold tests for sites in this study does not necessarily detract from the validity of the paleomagnetic results.

3.5-Paleomagnetic Results

Three of the four site groups (Greenfield, Quinado Canyon, San Antonio Reservior) indicated net clockwise rotations of 16.6 ± 17.2˚, 7.0 ± 10.8˚ and 17.0 ±19.1˚ respectively, while the fourth (Nacimiento River) indicated a small counterclockwise rotation of 3.8 ± 11.0˚. None of these groups indicated rotations larger than the calculated error (all errors calculated to the 95% level). Sample sizes were small (between 4 and 10 sites), which contributes to wide confidence interval. In addition, it should be noted that, while not significant within error, the 3 clockwise rotated groups are close to the limit for significance and probably indicate some element of actual clockwise rotation. The aggregate rotation for all 27 sites is 11.3˚ ± 8.8˚, indicating a statistically significant rotation of at least 2.5˚.

Group rotations indicate that some differences probably exist between groups, even those that are geographically close. The absence of rotation in the Nacimiento River region and its proximity to the San Antonio fault, a local thrust fault parallel to the Rinconada fault, indicated that this region may be different from the other three regions. Excluding this group from the aggregate site mean rotation yields a net rotation of 16.5˚ ± 9˚, a clockwise rotation of at least 7.5˚.

There is further evidence that variation in rotation amounts exist within groups. For samples within the Greenfield group, the mean rotation of sites located west of the Rinconada fault indicate a clockwise rotation of 20.6 ±16.6˚ - at least 4˚ of rotation-

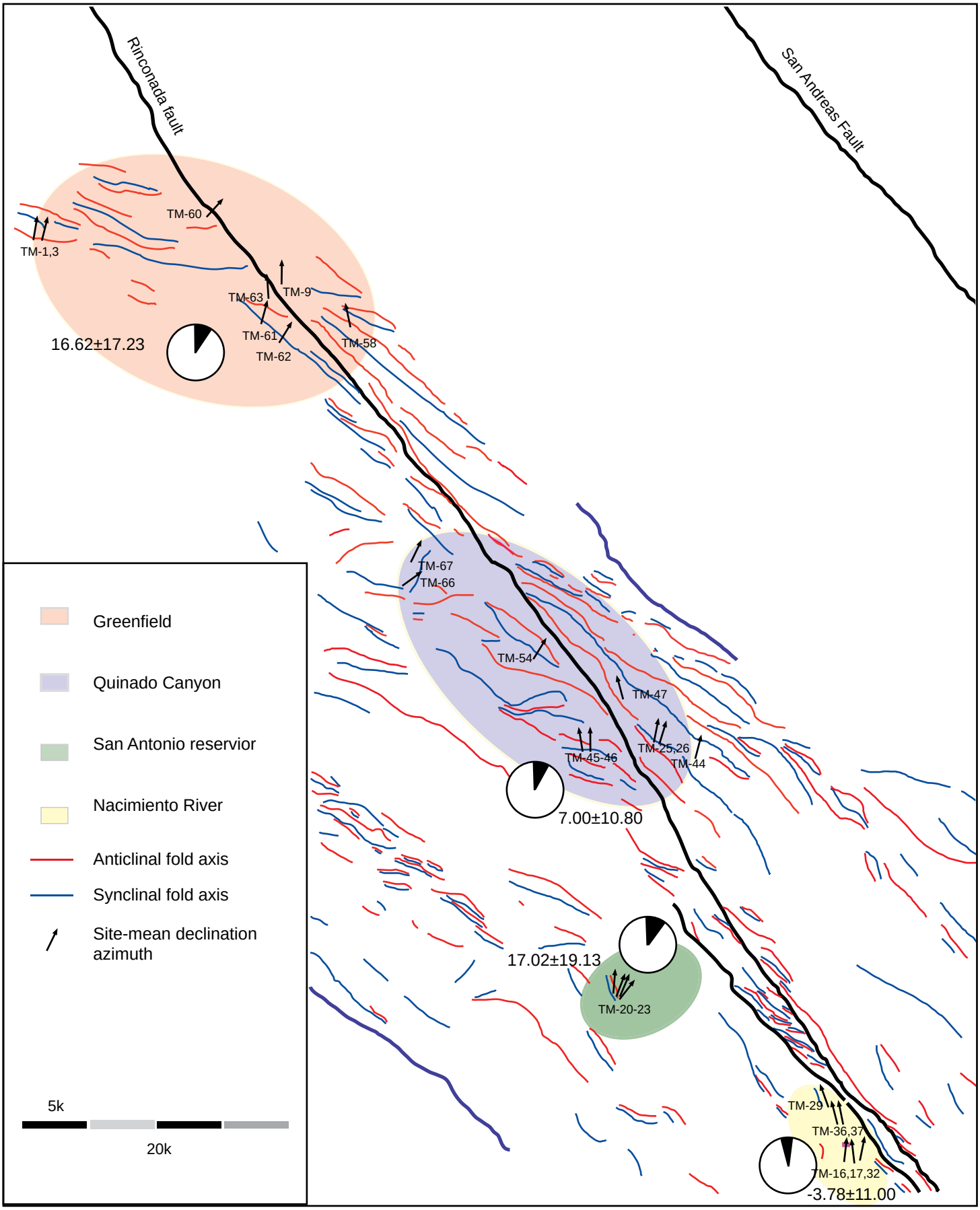

Figure 4. Map of study area showing paleomagnetic site groups and corresponding average rotations. Fold axes adapted from Dibblee (1976).

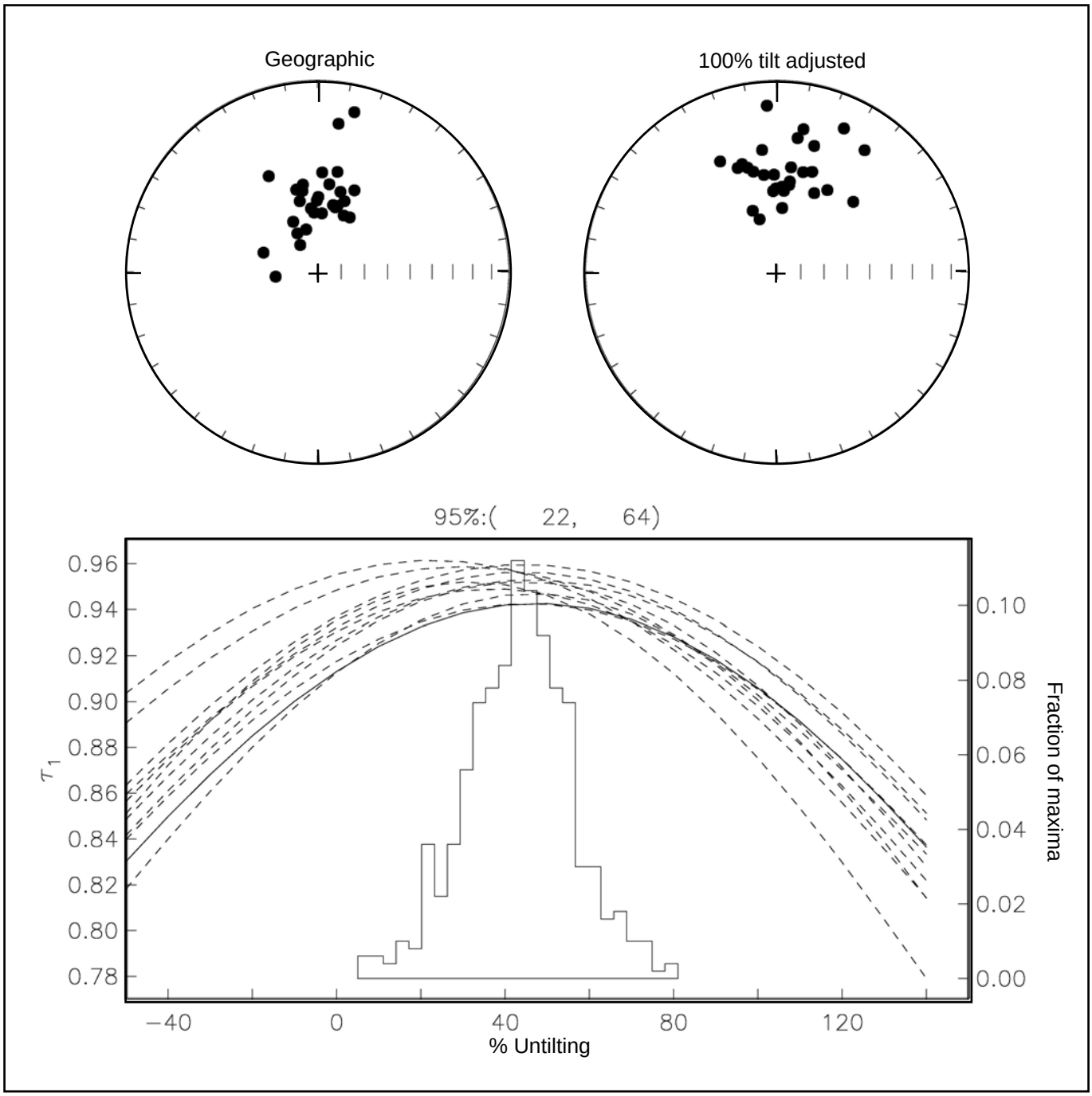

Figure 5. Lower hemisphere equal area projection of the 27 paleomagnetic site means used in this study. Reversed sites have been inverted through the origin to better show clustering. Site means do not cluster more closely after tilt adjustment. The graph indicates the result of Tauxe and Wilson (1994) paleomagnetic tilt test. The data peak at 45% untilting and therefore do not pass the tilt test.

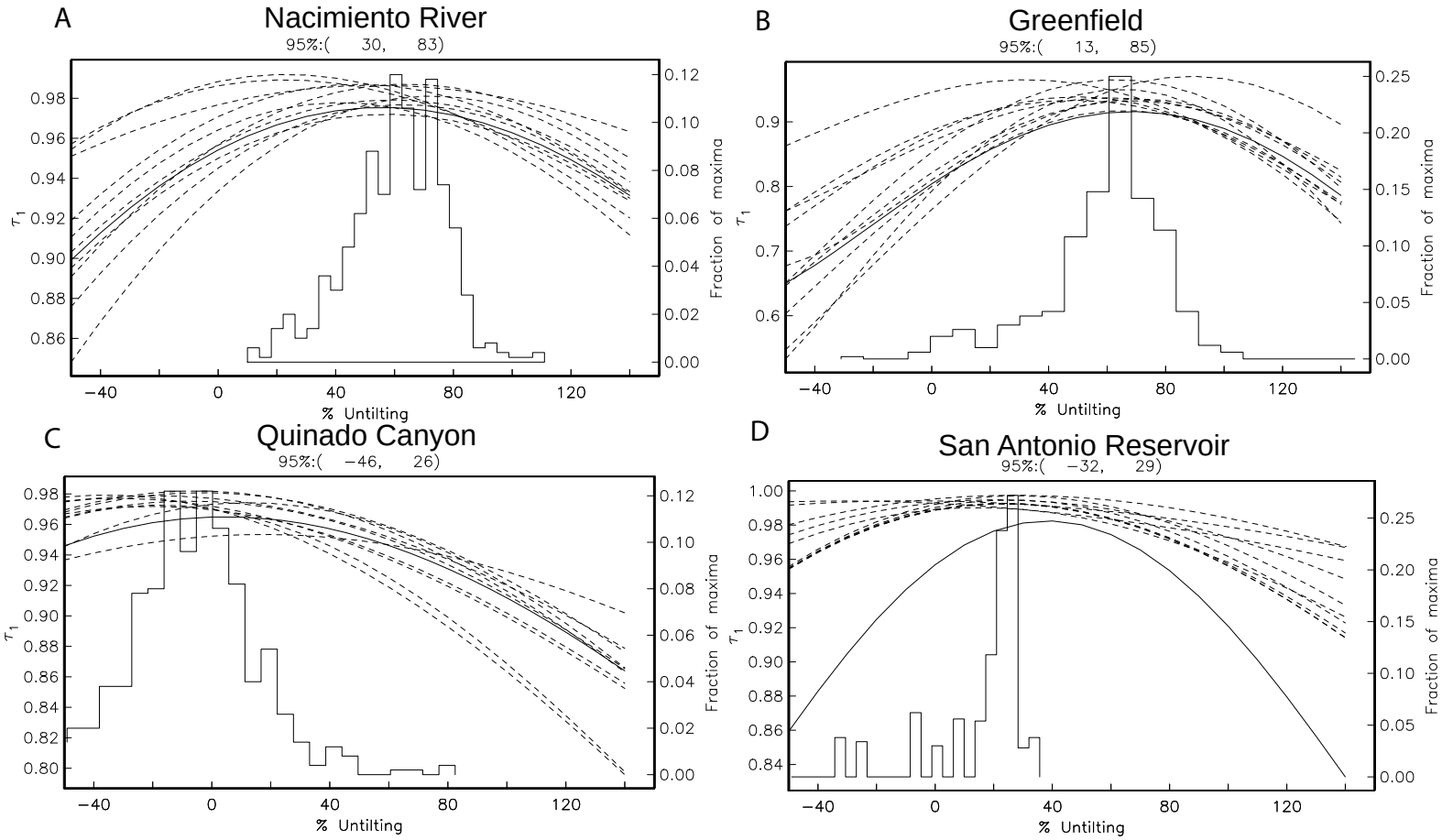

Figure 6. Results of Tauxe and Wilson fold test for four different grouped regions showing untilting of 60%, 65%, 0% and 25% in A-D.

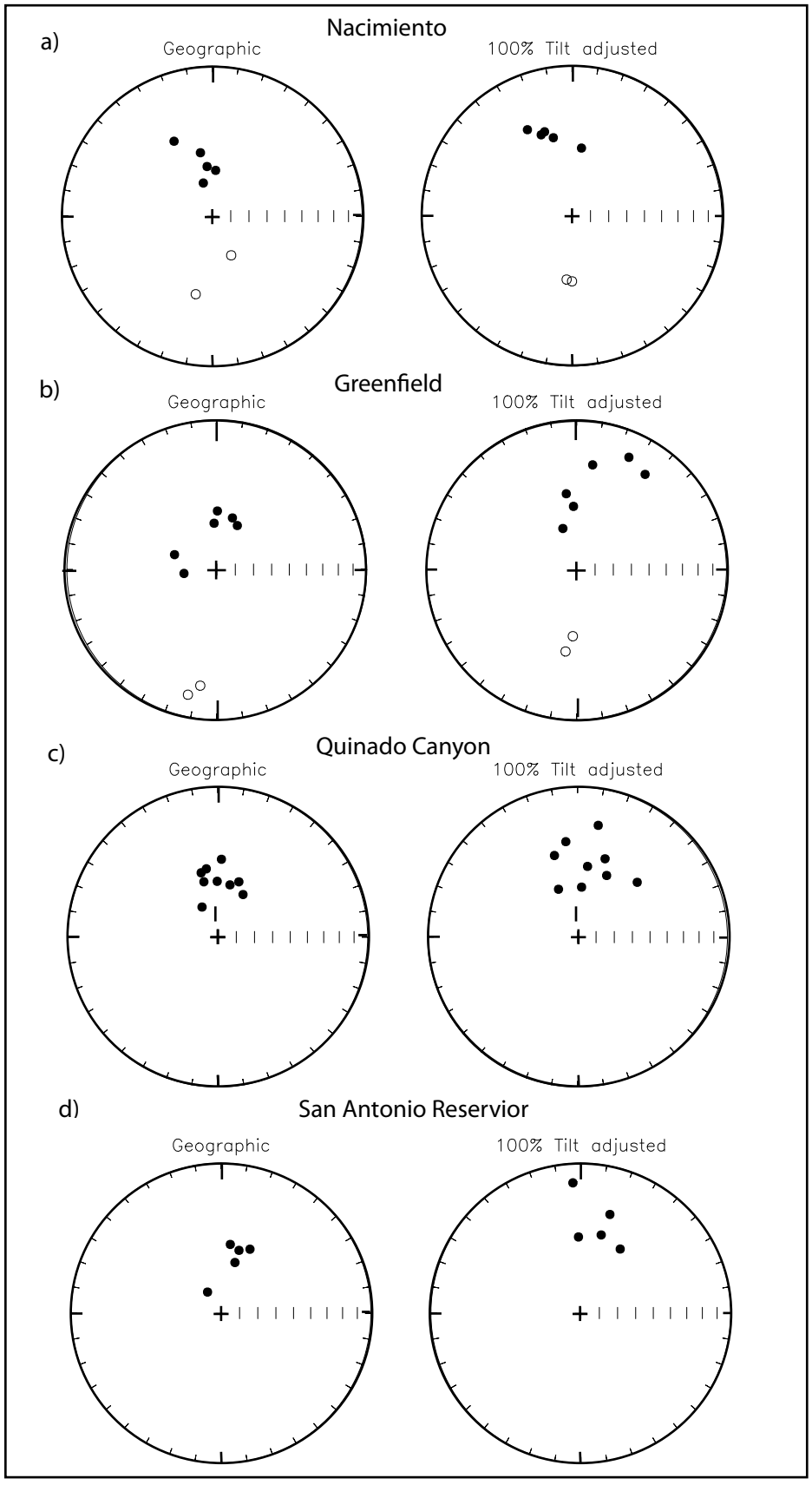

Figure 7. Equal area projection of paleomagnetic site mean directions. Unfilled circles indicate reversed polarity sites and filled circles are normal polarity sites.

Site	Declination	Inclination	a95	R (+ is Clockwise)	% error	Distance from fault (km)
1	3.19	53.35	4.6	9.7	8.17	10.3
3	7.7	44.2	6	14.2	8.6	10.3
9	357.2	55.3	9.7	-3.7	14.1	0.2
16	4.84	55.08	10.2	11.5	14.8	2.7
17	359.94	54.2	3.7	6.6	6	2.7
20	358.23	47.94	5.6	4.8	7.4	9.4
21	14.64	45.27	4.7	21.2	6.2	9.4
22	16.46	32	4.5	23.1	5.3	9.4
23	31.63	48.5	6.2	38.2	8.13	9.4
25	10.5	25.2	4.2	17.1	4.9	2.0
26	4.64	62.65	8.4	11.2	15.2	2.0
29	332.7	35.4	18.9	-20.7	19	1.1
32	346.6	45.31	16.8	-6.8	19.7	2.7
36	339.2	41.6	15.8	-14.2	17.4	2.0
37	342	40.5	11.3	-11.4	12.3	2.0
44	8.1	50.7	13.4	14.7	17.5	2.4
45	353	36.1	12.2	-0.4	12	2.1
46	344.2	42.9	15.9	-9.2	17.8	2.1
47	338.3	61.9	15.5	-15.1	27.8	1.2
54	25.3	52.5	9.9	31.9	13.5	1.8
58	341.6	66.4	4.8	-11.84	10.1	2.4
60	35.8	22.8	9.6	42.4	8.9	0.6
61	8.7	30	5.9	15.3	6.3	1.7
62	25	18.5	9.3	31.6	8.5	2.4
63	352.3	47.7	4.6	-1.1	6.3	0.5
66	47.5	45.1	7.2	54.1	8.8	5.2
67	19.3	43.9	9.8	25.9	11.4	4.8

Table 1. Results for all paleomagnetic sites with mapped distance from the Rinconada fault.

Region	At site Obliquity	Adjacent Folds Obliquity	Obliquity from Titus (2007)	Paleomagnetic Rotation
Greenfield	15.7	19	16 +/-16	16.6 +/- 17.2
Quinado Canyon	9.4	18	27 +/- 17	7+/-10.8
San Antonio Res.	8	16	24+/-11	17 +/- 19.1
Nacimiento River	-49	1	14+/-13	-3.8 +/-11

Table 2. Results of fold axis obliquity and Paleomagnetic rotation at each of 4 regions. Note that Nacimiento River section exhibits the least obliquity to the fault and also indicates no Paleomagnetic rotations.

while the two sites to the east of the Rinconada fault are not rotated or rotated slightly counterclockwise. This same pattern occurred within the Quinado Canyon group, where the 5 sites west of the Rinconada fault have a mean rotation of 12.6˚ while the 4 sites to the east had a mean rotation of 4.3˚. This finding of east-west differences is supported by site mean analysis of all 15 sites west of the Rinconada fault (excluding those in the Nacimiento River section) suggesting a mean clockwise rotation of at least 11.2˚ (20.5˚ ± 9.3˚). In contrast, sites east of the Rinconada fault indicate no significant rotation (clockwise 2.1˚ ±11.0˚).

4. Interpretations of Paleomagnetic Data

4.1- Comparison with Previous Studies

The rotation magnitudes reported in this study, 11.3 ± 8.8˚ clockwise for all 27 sites and 20.5 ± 9.3˚ clockwise for 15 sites west of the Rinconada fault, are consistent with the rotations from other previous nearby paleomagnetic studies. Titus et al. (2007) reported a clockwise rotation of 14 ± 7˚ for 11 sites that are included within the larger dataset used in this study. Omarzai (1996) reported a rotation of 14.4 ±5˚ at Horse Canyon near the Greenfield section of this study. The results of studies elsewhere in central California have also added to evidence for clockwise block rotations north of the Transverse Ranges. Extensive recent rotations of 35˚ to 55˚ to the northwest of this study area are observed by Holm et al. (1991) adjacent to the San Gregorio fault zone. Other paleomagnetic studies in south-central California (Greenhaus and Cox, 1979; Terres, 1984; Ellis et al., 1993; Onderdonk, 2005) indicate rotations of 49˚ on the coast (Greenhaus and Cox, 1979) and 20-45˚ in the interior basins (Fig. 8).

In addition to total rotations, it is also important to examine the rate of rotation over time. The age of onset of transpression differs across study areas; consequently, the rates of rotation may yield more accurate comparison between study areas than overall rotation magnitude of rotation. Rotations adjacent to the San Gregorio fault zone are constrained to the last 2.5 million years and indicate extremely high rotation rates of 15˚ to 20˚ per million years. This rate of rotation is significantly higher than the 3-6˚ per million year rates reported in southern California (Jackson and Molnar, 1990).

The results from this study and other rotations in the Rinconada fault zone do not predict rotation rates as high as those reported along the San Gregorio fault zone, however, rotations are probably closer to half the magnitude of rotations observed in southern California. Assuming a conservative estimate of 10˚ overall rotation and constraint of onset of transpression to between 5 and 8 Ma, rotations of 1.5-2˚ per million years are plausible. Due to the parallel fault geometry in central California and the expectation that a purely compressional tectonic environment would not cause such significant rates of rotation, it follows that some degree of fault parallel motion is accommodated off-fault (McKenzie and Jackson, 1982; Argus and Gordon, 2001; Titus et al, 2006).

4.2-Implications for Crustal Blocks

The differences between site mean rotations suggest that the sites east (rotated clockwise 2.1˚ ±11.0˚) and west (rotated clockwise 14.0˚ ±16.1˚) of the Rinconada fault are located on different crustal blocks which differ significantly in magnitudes of rotation. In addition, sites in the Nacimiento River region indicate no significant rotation and are probably located on a separate crustal block from the other regions. Rotations

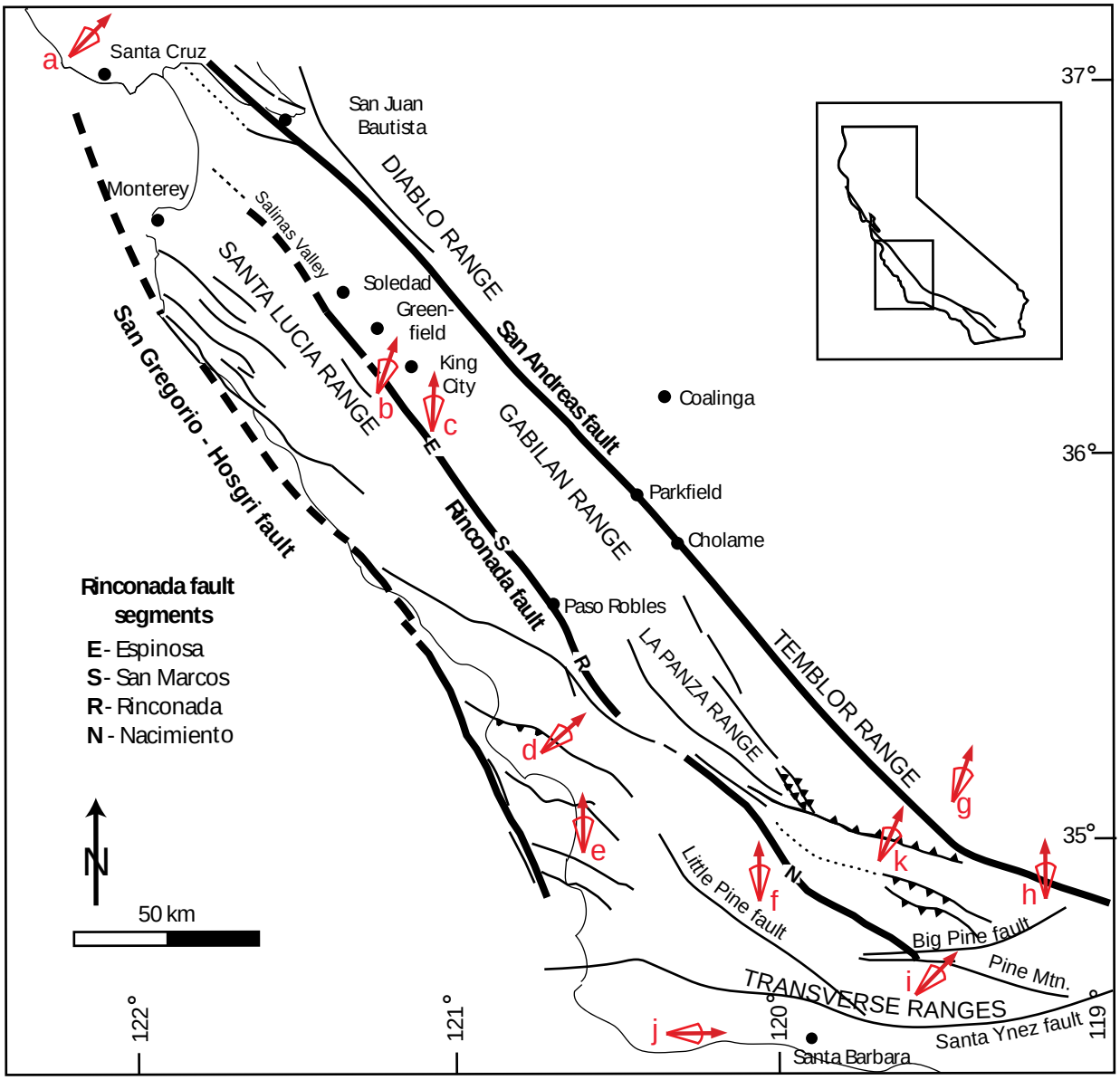

Figure 8. Map of central California with major faults and block rotations from previous studies. Red arrows indicate declination deflection from north. (A) Clockwise rotations of 35-55˚ near Santa Cruz (Holm et al., 1991). (B,C) Clockwise rotations of 20.5˚ and 3.8˚ from this study. (D) Clockwise rotations of 49˚ near Morro Bay (Greenhaus and Cox, 1979). (E) No significant rotation at Lions Head (Luyendyk et al. 1985). (F) No significant rotation at Figueroa Mtn (Onderdonk, 2005) (G,H)Possible rotation 6.4˚ in Lockwood valley (Terres, 1984). (I) Clockwise rotations of 40˚ near western Big Pine Fault (Onderdonk, 2005). (J) 90˚ clockwise rotation of Santa Ynez region (Luyendyk et al., 1985). (K) Clockwise rotations of 23˚ in Cuyama Basin (Ellis et al. 1993)

within the Greenfield region indicate rotations that decrease with distance from the Rinconada fault. This may imply that rotational blocks are small in scale, or that there is a continuous gradient of deformation in which blocks are modeled as infinitesimal in scale.

4.3- Kinematic Models of Vertical Axis Rotation

Models for rotation throughout southern California typically call upon large rigid crustal blocks that are bounded by pairs of right and left lateral strike-slip faults; faults that are generally thought necessary to accommodate rotation differences between blocks (Dibblee, 1976; Luyendyk et al. 1980). Rigid block rotation is a common assumption for examining vertical axis rotations expressed by declination anomalies. However, the block size, geometry and bounding surfaces of crustal blocks vary considerably in different models (McKenzie and Jackson, 1982; Luyendyk, 1985; Lamb, 1987; Molnar, 1992; Sonder et al., 1994). Block rotation, can occur either passively due to deformation in the lower lithosphere, or actively as a result of shear on the surface (Molnar, 1992).

There are a number of models by which paleomagnetic rotations are interpreted. Differences between these kinematic models are rooted in assumptions for block geometry, the relationship between observed rotations and the surrounding velocity field and the relationship between rotation and proximity with the adjacent fault. A kinematic model can never be expected to perfectly match observations from the field, but instead can be useful for the simplification of these complex processes. Below, I describe several models of paleomagnetic rotation that may be applicable to the study area and compare them to the observed data.

A “domino block’ model proposed by McKenzie and Jackson (1982) is based on relatively large blocks with sizes similar to the order of magnitude to the deforming zone (Fig. 9). Blocks are parallel to one another and have rotations of equal magnitude. Rotation of the fault blocks is accommodated by intersecting sinistral and dextral faults that strike obliquely to each other. This model predicts that rotation rates for large blocks spanning the entire deforming zone are double those of smaller blocks within, but not bounding, the deforming zone. Rotations in southern California are thought to take place on large fault blocks that generally are congruent with this rotational model.

An improvement to the “domino block” model is provided by Lamb (1987), who, in his model accounts for size and shape of crustal blocks. Rotation magnitudes are found to be largely influenced by geometry of rotation blocks (Lamb, 1987). Lamb reinterprets rotation with consideration for the aspect ratio, or ratio between the long and short axis of the rotating block. When the geometry of blocks is taken into consideration, elongate blocks are more resistant to rotation compared to equidimensional blocks. Support for geometrically dependent rotations is observed in southern California, where rotations are less than those predicted by the tectonic setting (McKenzie and Jackson, 1982) and fault blocks are predominately elongate. (Luyendyk et. al, 1985; Lamb,1987). Another feature of Lamb’s complex block rotation model is that rotations behave along a continuum of shear that dissipates with distance from the fault (Fig. 9). Based on this feature, rotations of blocks nearer to the main fault are predicted to be larger than those further away (Lamb, 1987).

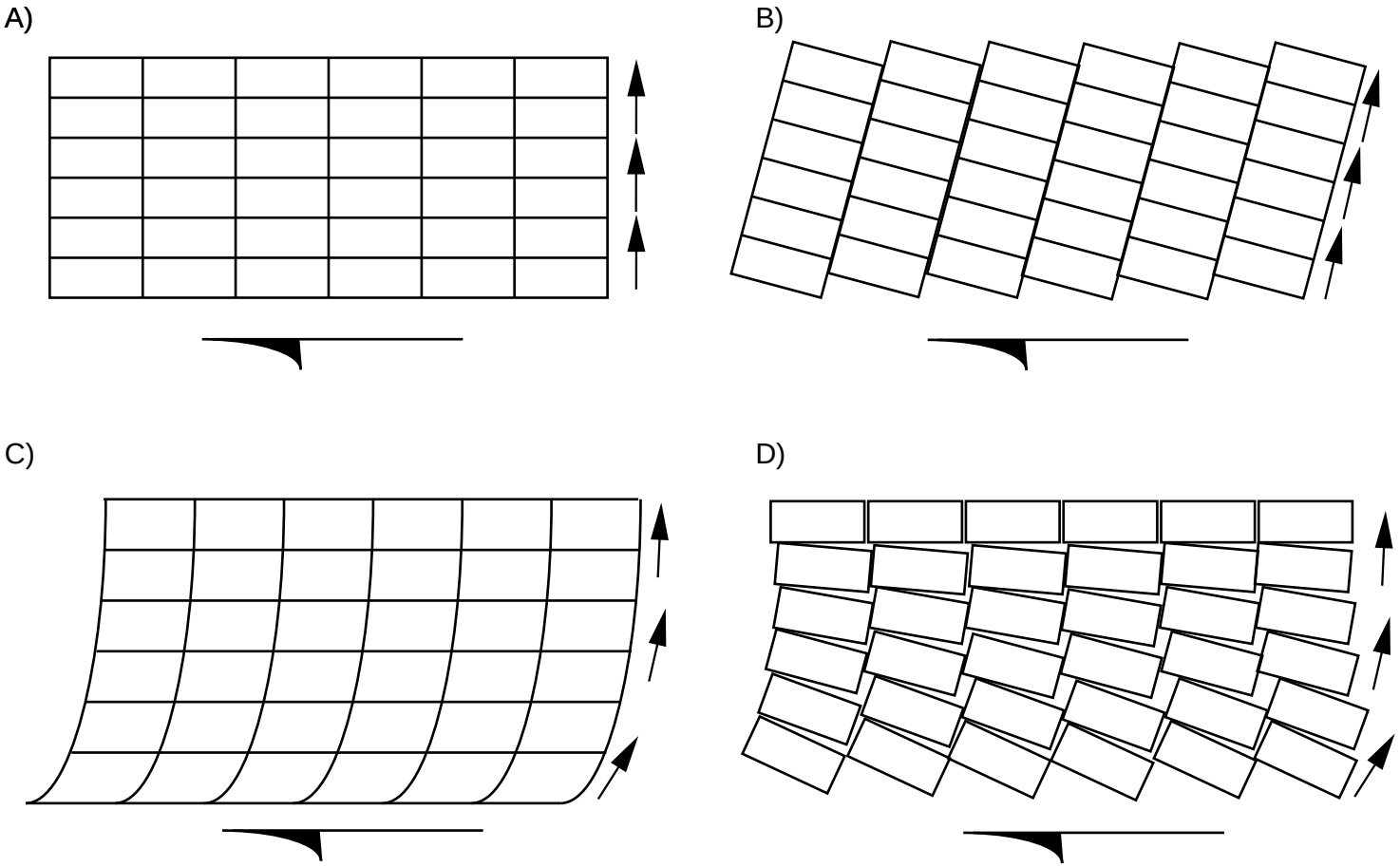

Figure 10. Diagrams of kinematic models that accommodate transcurrent deformation. Large arrows indicate sense of motion and small arrows indicate predicted paleomagnetic rotation from north (up). (A) Undeformed crustal block. (B) Domino block model similar to model by McKenzie and Jackson (1983). Note that left-lateral faulting is predicted between blocks and blocks rotate equally (both laterally and with distance from fault). (C) Pervasive continuum deformation model. Blocks are deformed and rotate increasingly with proximity to the fault. (D) Small block continuum model. Blocks are undeformed, but rotations increase with proximity to the fault. Note that with small block size, this model approximates (C). Modified from Sonder et al. (1994)

Observations in the field confirm many of the predictions of the Lamb (1987) rotational model (Sonder et al. 1994). In the particular example Las Vegas valley shear zone, a system which may be analogous to the Rinconada fault zone, Sonder et al. conclude that the rotational blocks are relatively small and are not necessarily fault bounded. Estimates of fault blocks size are approximately 2-4 km wide at a maximum, nearly an order of magnitude smaller than estimates made in previous models (Sonder et al. 1994). In addition, rotations in the Las Vegas shear zone are systematically related to distance from the fault. Sonder et al. discover clockwise rotations reaching 92-100˚ in the localities closest to the shear zone, intermediate rotations from 30-80˚ from locations 1-6 km from the shear zone, and rotations ranging from 6˚ counterclockwise to 23˚ clockwise at distances greater than 10 km from the shear zone.

4.4- Comparing Kinematic Models to Results in Central Californa

Even though the rotations found in central California are small, they are difficult to explain using standard kinematic models. There are no left-lateral faults observed near the Rinconada fault that could accommodate motion between blocks or suggest possible boundaries for fault blocks. In addition, rotations are significantly different even between sites that are geographically close – indicating both that fault blocks may be bounded by small-scale deformational features and that rotational blocks may be significantly smaller than sizes predicted by McKenzie and Jackson (1982). Within the Quinado Canyon section of this study, sites that are less than 2 kilometers apart (67 and 68; 25 and 47) have differences in declination direction that are nearly 30˚ apart. These findings suggest that block sizes may be as small, similar to block sizes of 2-4 km reported in the Las Vegas Valley shear zone (Sonder et al. 1994).

In addition, data from the Greenfield section suggest that rotation magnitudes are higher at locations near the fault than away from the fault. At sites ~10 km from the Rinconada fault, sites 1 and 3 were rotated clockwise 9.7 and 14.2˚. At ~2 km from the fault (sites 61 and 62), declination rotations of 15.3 and 31.6˚ were observed and at site 9 and 60, ~0.5 from the Rinconada fault, rotations of 42.4˚ and 4˚ were observed. These observations support deformation that behaves along a continuous shear zone with higher rotations nearer to the major fault.

4.5- Comparison between Crustal Block Rotations and Fold Axis Orientation

Distributed deformation in the form of en echelon transpressional folding is a source of strain accommodation adjacent to the Rinconada fault (Titus et al., 2007), an area dominated by moderately dipping upright folds. In a purely contractional system, folds initiate parallel to fault strike and remain in that orientation during deformation. In wrench tectonic system (where maximum stress is parallel to fault strike), folds initiate at 45˚ and rotate towards parallel. Transpression, which includes all intermediate maximum stress directions, causes folds which initiate at an angle less than 45˚ from fault strike and rotate towards parallelism while also undergoing compression and steepening of limb dips. Kinematic models of fold geometry (Jamison, 1991; Krantz, 1995) and their relation to stress orientation have been successful in quantifying transpressional deformation.

The fold axes mapped in central California are systematically oblique to the Rinconada fault by an average of 19˚± 17˚ (Titus el at., 2007) based on mapping by Dibblee (1976). Folds analyzed by Titus et al. (2007) are interpreted as initiating in a transpressional system due to the observed obliquity and fold hinge elongation.

The mapped fold orientations in central California are an expression of the same deformation that has caused the paleomagnetic rotations discussed in this paper. The Nacimiento River section, which lacks of clockwise paleomagnetic rotations observed in the other regions, also exhibits fold axis orientation that is much less oblique to the Rinconada fault than observed in the rest of the study area. Mapped folds surrounding this region (Titus, 2007) are oblique to the Rinconada fault by 14 ± 13 degrees and oblique by 18.8 degrees at a radius of 15km surrounding the site region (Mark Dyson, personal communication). Folds directly adjacent (within 5 km) to the Nacimiento River section were nearly parallel to fault strike at an obliquity of one degree. In locations near the other paleomagnetic regions (Greenfield, Quinado Canyon and San Antonio Reservoir), Titus et al. observe angles of obliquity approximately 8˚ higher (16±16˚, 27±17˚and 24±11˚, respectively). Adjacent mapped fold and estimates from Dyson (personal communication) indicate similar trends (Table 2).

These observations suggest that a significant relationship between rotation magnitudes and fold axis orientations exists, and may also explain the lack of rotations in the Nacimiento River section, which may be part of a block that is more resistant to transcurrent deformation and therefore shows signs of compression dominated deformation.

5. Discussion

5.1- Strain Partitioning Along the San Andreas Fault System

Previous research has suggested that transpression in a wrench dominated convergent setting is likely to partition oblique strain between subparallel strike-slip faults (Fig.10; Tikoff and Tessier, 1994). The degree to which strain is partitioned into

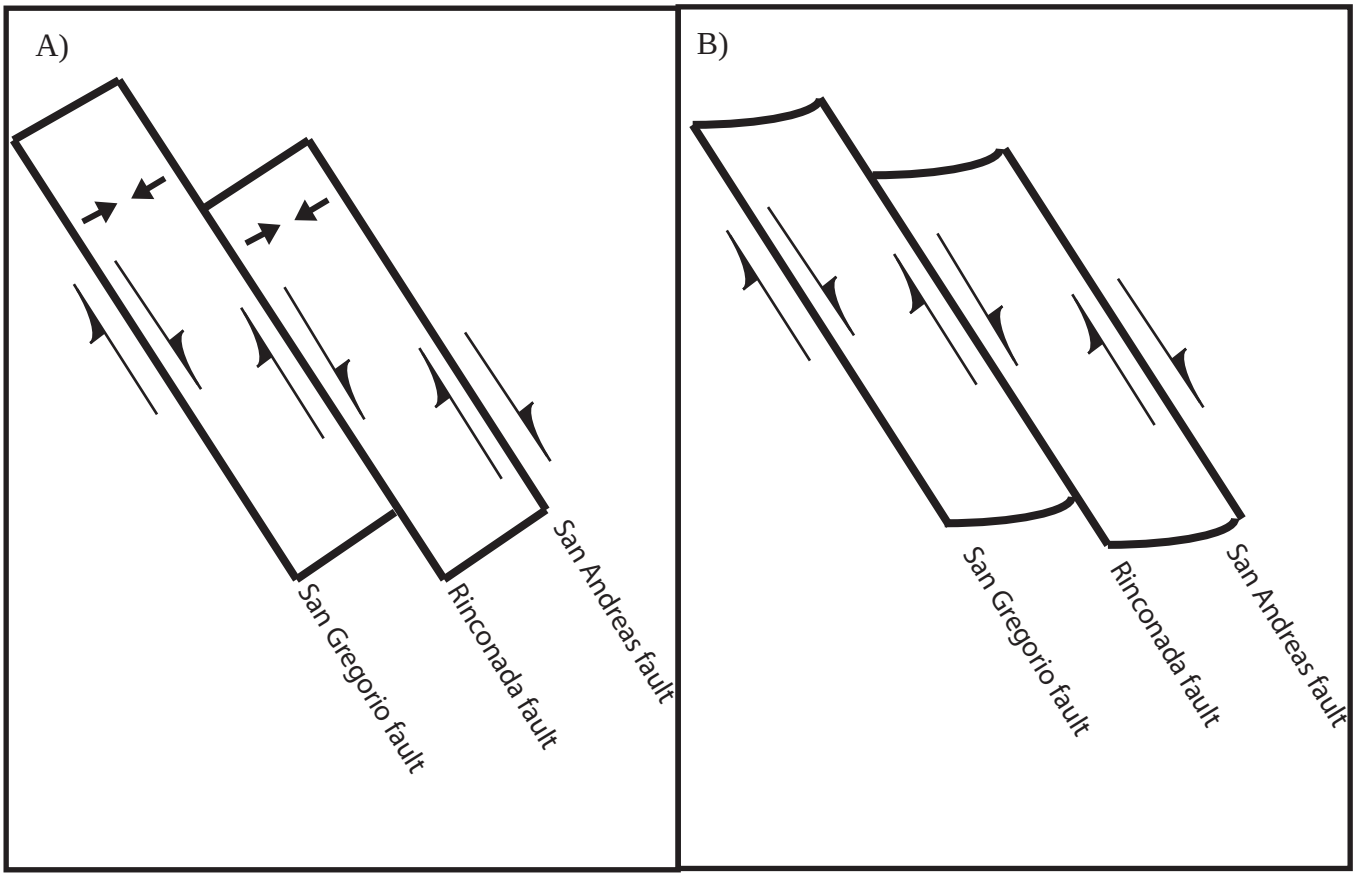

Figure 10. Models of strain partitioning in central California. (A) 100% strike-slip partitioned deformation All transcurrent motion occurs on major faults and all contraction occurs between faults. (B) Areas between faults accommodate some degree of transcurrent motion.

convergent and strike-slip components on faults and between faults is the subject of some debate (Mount and Suppe, 1987; Zoback et al. 1987; Tikoff and Tessier, 1994; Jones and Tanner, 1995).

At one extreme, strain is 100% partitioned neatly between fault parallel slip and fault normal convergence. In this model, all strike slip motion is accommodated along faults and all contraction is taken up between faults. Fold axis orientations within central California are interpreted in some research (Mount and Suppe, 1987 ; Zoback et at. 1987) as subparallel to fault strike (based on an angle of obliquity of 12˚). This is considered as evidence of a direction of stress away from the fault that is nearly fault normal, implying a primarily compressional environment away from the fault.

Other theories of strain partitioning allow for some element of transcurrent motion accommodated by off fault deformation. This model for strain accommodation is supported by the interpretations of low angle obliquity of central California folds observed by Jamison (1991) in which oblique fold axes are interpreted as rotations towards parallelism with fault strike and axial extensions. Fold axis orientation and fold geometry in central California was independently measured and indicated obliquity to the Rinconada fault of approximately 20˚ and suggested a 20-50˚ angle of oblique convergence adjacent to the fault (Titus et al., 2007). Correlations between fold axis obliquity near clockwise site and group block rotations from this paper offer support for this interpretation of off fault deformation accommodation.

5.2-Implications for San Andreas Fault Zone

Crustal block rotations of greater than 90˚ clockwise have been measured in southern California (Luyendyk, 1985). These rotations occur along a broad shear zone of

distributed deformation (Luyendyk, 1985; Molnar,1992) approximately 130 km wide throughout the San Andreas fault system. Rotation magnitudes in central California, while clearly different than those in southern California, are still inconsistent with models that suggest that oblique convergence is partitioned with almost all fault parallel motion (strike-slip) taken up along faults and all fault perpendicular motion (compression) taken up away from the fault. The clockwise rotations found in this study were collected from sites within 10 km of the Rinconada fault. These rotations, at least 10˚ at sites west side of the Rinconada fault, suggest that within this zone there is some element of transcurrent off-fault deformation. Other rotations found in central California along the San Gregorio fault zone indicate that block rotations are prevalent throughout the San Andreas fault zone in central California and are not isolated to areas adjacent to the Rinconada fault.

Rotations found in this study and elsewhere (Holm,1991; Omarzai, 1996; Titus, 2007) could determine how deformation is accommodated, however, considerably more data will need to be collected before we can look at spatial variations in block rotation magnitude to accurately determine block size and degree of strain partitioning.

Conclusions

In this study, clockwise rotations of 11.3 ± 8.8˚ were found throughout the study area and a mean rotation of at least 11.2˚ (20.5˚ ± 9.3˚) was found for 15 sites west of the Rinconada fault. These paleomagnetic results are consistent with previous estimates of rotation (Omarzai, 1996) and are taken as evidence for some transcurrent motion accommodated between faults in the San Andreas fault system. Comparison with mathematical models for rotation (McKenzie and Jackson, 1982; Lamb 1987; Sonder, 1994) indicate that rotating blocks along the Rinconada fault are probably small, not

bounded by faults and rotate independently. Block rotations are probably influenced strongly by distance from the Rinconada fault and by individual fault geometry. Rotations adjacent to the Rinconada fault zone are indicative of distributed off fault deformation and support the hypothesis that transpression does not partition into purely strike-slip and dip-slip components of deformation throughout the San Andreas fault zone. Instead, areas between parallel faults in central California are affected by convergent wrenching that must be considered when studying how plate boundary deformation is accommodated.

6. Acknowledgements

I would like to thank all those involved in the collection of the data used in this paper. Paleomagnetic cores that were used in this data set were collected by Bernie Housen, Eric Horsman, Basil Tikoff, and Sarah Titus between 2004 and 2007. I would like to also thank Eric Horsman for showing me how to drill paleomagnetic cores and for helping in all aspects of fieldwork, Paul Riley for his help during drilling, and Bernie Hausen and Russell Burmester at the University of Western Washington for their helpful expertise and access to UWW's paleomagnetic laboratory. Thank you to Mark Dyson for using his personally designed program to analyze fold obliquity. I am also especially grateful for the help of Sarah Titus, who began this project and helped me through all aspects of planning, research and (especially) editing.

Lastly, I would like to thank the Carleton College Geology Department and the entire faculty for their assistance and support throughout the comps process.

7. References

Argus, D. F. D., and Gordon, R. G. R., 2001, Present tectonic motion across the Coast Ranges and San Andreas fault system in Central California: Geological Society of America Bulletin, v. 113, p. 1580-1592.

Atwater, T. T., 1970, Implications of plate tectonics for the Cenozoic tectonic evolution of western North America: Geological Society of America Bulletin, v. 81, p. 3513-3535.

Atwater, T. T., and Stock, J., 1998, Pacific-North America plate tectonics of the Neogene southwestern United States; an update: International Geology Review, v. 40, p. 375-402.

Beck, M. E. M., 1980, Paleomagnetic record of plate-margin tectonic processes along the western edge of North America: Journal of Geophysical Research, v. 85, p. 7115-7131.

Burchfiel, B. C., Cowan, D. S., and Davis, G. A., 1992, Tectonic overview of the Cordilleran Orogen in the Western United States The Cordilleran Orogen; conterminous U.S, 407-479 p.

Butler, R. F. R., 1992, Paleomagnetism; magnetic domains to geologic terranes, 319 p.

Cox, A. A., Doell, R. R., and Dalrymple, G. B., 1963, Geomagnetic polarity epochs and Pleistocene geochronometry: Nature, v. 198, p. 1049-1051.

Cox, A. A., Doell, R. R., and Dalrymple, G. B., 1964, Reversals of the earth's magnetic field: Science, v. 144, p. 1537-1543.

Cox, A. A., Doell, R. R., and Dalrymple, G. B., 1968, Time scale for geomagnetic reversals: The history of the Earth's crust, a symposium--Goddard Inst. Space Studies, 1966, Conf. Contr, 101-108 p.

Crowell, J. C., 1962, Displacement along the San Andreas fault, California: Special Paper- Geological Society of America, pp. 61.

Dibblee, T. W., Jr., 1976, The Rinconada and Related Faults in the Southern Coast Ranges, California, and Their Tectonic Significance: Geological Survey Professional Paper, vol. 981, pp. 55.

Ellis, B. J. B., Shaul, L., and Yeats, R. S., 1993, Magnetic stratigraphy of the Morales Formation; late Neogene clockwise rotation and compression in the Cuyama Basin, California Coast Ranges: Tectonics, v. 12, p. 1170-1179.

Fisher, R., 1953, The Expansion of Statistics: Journal of the Royal Statistical Society. Series A. Statistics in Society, v. 116, p. 1-10.

Greenhaus, M. R., and Cox, A. A., 1979, Paleomagnetism of the Morro Rock-Islay Hill complex as evidence for crustal block rotations in central coastal California: Journal of Geophysical Research, v. 84, p. 2393-2400.

Gross, M. R. M., 1995, Fracture partitioning; failure mode as a function of lithology in the Monterey Formation of coastal California: Geological Society of America Bulletin, v. 107, p. 779-792.

Holm, E. J. E., Horns, D. M., and Verosub, K. L., 1991, Rapid post-Miocene tectonic rotation associated with the San Gregorio fault zone in Central California: Geophysical Research Letters, v. 18, p. 2213-2216.

Hornafius, J. S. J., 1985, Neogene tectonic rotation of the Santa Ynez Range, western Transverse Ranges, California, suggested by paleomagnetic investigation of the Monterey Formation: Journal of Geophysical Research, v. 90, p. 12.

Jackson, J. J., and Molnar, P. P., 1990, Active faulting and block rotations in the western Transverse Ranges, California: Journal of Geophysical Research, v. 95, p. 22.

Jamison, W. R. W., 1991, Kinematics of compressional fold development in convergent wrench terranes: Tectonophysics, v. 190, p. 209-232.

Jones, R. R., and Tanner, P. W. G., 1995, Strain partitioning in transpression zones: Journal of Structural Geology, v. 17, p. 793-802.

Kamerling, M. J., and Luyendyk, B. P., 1979, Tectonic rotations of the Santa Monica Mountains region, western Transverse Ranges, California, suggested by paleomagnetic vectors: Geological Society of America bulletin, v. 90, p. 331.

Krantz, R. W., 1995, The transpressional strain model applied to strike-slip, oblique-convergent and oblique-divergent deformation: Journal of Structural Geology, v. 17, p. 1125-1137.

Lamb, S. H., 1987, A model for tectonic rotations about a vertical axis: Earth and Planetary Science Letters, v. 84, p. 75-86.

Lisowski, M. M., Savage, J. C., and Prescott, W. H., 1991, The velocity field along the San Andreas Fault in Central and Southern California: Journal of Geophysical Research, v. 96, p. 8369-8389.

Luyendyk, B. P., Kamerling, M. J., and Terres, R. R. R., 1980, Geometric model for Neogene crustal rotations in southern California: Geological Society of America Bulletin, v. 91, p. 211.

Luyendyk, B. P. B., Kamerling, M. J., Terres, R. R. R., and Hornafius, J. S. J., 1985, Simple shear of Southern California during Neogene time suggested by paleomagnetic declinations: Journal of Geophysical Research, v. 90, p. 12.

McKenzie, D. D., and Jackson, J. J., 1983, The relationship between strain rates, crustal thickening, palaeomagnetism, finite strain and fault movements within a deforming zone: Earth and Planetary science Letters, v. 65, p. 182-202.

McKenzie, D. P. D., and Parker, R. L., 1967, The north Pacific; an example of tectonics on a sphere: Nature, v. 216, p. 1276-1280.

Molnar, P. P., 1992, Brace-Goetze strength profiles, the partitioning of strike-slip and thrust faulting at zones of oblique convergence, and the stress-heat flow paradox of the San Andreas Fault Fault mechanics and transport properties of rocks; a festschrift in honor of W. F. Brace, 435-459 p.

Morgan, W., 1968, Rises, trenches, great faults, and crustal blocks: Journal of Geophysical Research, v. 73, p. 1959-1982.

Mount, V. S. V., and Suppe, J., 1987, State of stress near the San Andreas Fault; implications for wrench tectonics: Geology, v. 15, p. 1143-1146.

Namson, J. S., and Davis, T. L., 1988, Seismically active fold and thrust belt in the San Joaquin Valley, Central California: Geological Society of America Bulletin, v. 100, p. 257-273.

Omarzai, S. K., 1996, Paleomagnetism Applied to the Monterey Formation of California: Ph.D. thesis, University of California Santa Cruz.

Onderdonk, N. W. N., 2005, Structures that accommodated differential vertical axis rotation of the western Transverse Ranges, California: Tectonics, v. 24, p. 15.

Page, B. M., 1981, The southern Coast Ranges; The geotectonic development of California: Rubey, v.1, p. 329-417.

Prentice, C. S. C., 1989, The northern San Andreas Fault; Russian River to Point Arena Sedimentation and tectonics of western North America; v. 2, The San Andreas Transform Belt, p. 49-51.

Sonder, L. J. L., Jones, C. H., Salyards, S. L., and Murphy, K. M., 1994, Vertical axis rotations in the Las Vegas Valley shear zone, southern Nevada; paleomagnetic constraints on kinematics and dynamics of block rotations: Tectonics, v. 13, p. 769-788.

Tauxe, L., and Watson , G. S., 1994, The fold test; an eigen analysis approach: Earth and Planetary Science Letters, v. 122, p. 331-341.

Terres, R. R. R., 1984, Paleomagnetism and tectonics of the central and eastern Transverse Ranges, Southern California, 364 pp.

Terres, R. R. R., and Luyendyk, B. P., 1985, Neogene tectonic rotation of the San Gabriel region, California, suggested by paleomagnetic vectors: Journal of Geophysical Research, v. 90, p. 12.

Tikoff, B. B., and Teyssier, C., 1994, Strain modeling of displacement-field partitioning in transpression orogens: Journal of Structural Geology, v. 16, p. 1575-1588.

Titus, S., DeMets, C., and Tikoff, B., 2006, Thirty-five-year creep rates for the creeping segment of the San Andreas Fault and the effects of the 2004 Parkfield earthquake; constraints from alignment arrays, continuous Global Positioning System, and creepmeters: Bulletin of the Seismological Society of America, v. 96, p. 250-268.

Titus, S. J. S., Housen, B., and Tikoff, B., 2007, A kinematic model for the Rinconada fault system in central California based on structural analysis of en echelon folds and paleomagnetism: Journal of Structural Geology, v. 29, p. 961-982.

Vine, F. J., and Mathews, D. H., 1963, Magnetic anomalies over oceanic ridges: Nature, v. 199, p. 947-949.

Zoback, M. D. M., Zoback, M. L., Mount, V. S., Suppe, J., Eaton, J. P., Healy, J. H., Oppenheimer, D. H., Reasenberg, P. A., Jones, L. M., Raleigh, C. B., Wong, I. G., Scotti, O., and Wentworth, C. M., 1987, New evidence on the state of stress of the San Andreas fault system: Science, v. 238, p. 1105-1111.